The Folding and Stability of Titin Immunoglobulin-Like Modules, with Implications for the Mechanism of Elasticity

Anastasia S. Politou, David J. Thomas, and Annalisa Pastore
European Molecular Biology Laboratory, 69012 Heidelberg, Germany

ABSTRACT Titin (first known as connectin) is a vast modular protein found in vertebrate striated muscle. It is thought to assist myofibrillogenesis and to provide a passive elastic restoring force that helps to keep the thick filaments properly centered in the sarcomere. We show that representative titin modules do indeed fold independently, and report their stabilities (i.e., ΔG of unfolding and melting temperature) as measured by circular dichroism, fluorescence, and nuclear magnetic resonance spectroscopies. We find that there is a region-dependent variation in stability, although we find no evidence to support a proposed elastic mechanism based on a molten-globular-like equilibrium folding intermediate, nor do our calculations support any mechanism based on the configurational entropy of the molecule itself; instead we suggest a model based on hydrophobic hinge regions that would not be strongly dependent on the precise folding pattern of the chain.

INTRODUCTION

The wealth of sequences published in recent years and the large number of tertiary structures determined have revealed a constantly expanding class of "modular" proteins, i.e., proteins composed of one or more types of repeated structural and functional units. The component modules discovered so far can be classified as belonging to a few structural superfamilies with very similar tertiary structures but often very highly divergent sequences. It seems that a critical number of highly conserved residues form the structural scaffold of each superfamily and account for the similar packing of its members, whereas the rest can diverge to allow for new, specialized functional rôles. Similarly folded protein modules can, however, clearly have different stabilities (Novokhatny and Ingham, 1994; Politou et al., 1994b). Overall, the picture that emerges for the structural superfamilies is that of groups of protein modules with very conserved packing but very divergent sequences and stabilities.

One of the most striking examples of modular proteins is the vast muscle protein titin, first known as connectin. Titin is the largest protein described to date (~3 MDa) and the third most abundant component of the sarcomere in vertebrate striated muscle (Maruyama et al., 1984; Wang, 1985; Kurzban and Wang, 1988; Fürst et al., 1988; Maruyama, 1994; Trinick, 1994; Keller, 1995). Single titin molecules are ~1 μm long and span half the sarcomere, with the N-terminus and the C-terminus located in the Z-disc and the M-line, respectively (Fürst et al., 1988; Nave et al., 1989; Labeit et al., 1992). The functions of titin vary along its length: in the I-band it is believed to act as an elastic connection between the thick filaments and the Z-disc (Fürst et al., 1988; Horowits et al., 1989; Funatsu et al., 1993); in the A-band it is closely associated with myosin and the other constituents of the thick filament (Labeit et al., 1992; Soteriou et al., 1993b); in the M-line it forms an integral part of an extensive protein meshwork (Vinkemeier et al., 1993; Gautel et al., 1993). Because of these multiple interactions, titin is thought to play an important role in providing sarcomere alignment during muscle contraction and in aiding the assembly and regulating the precise length of the thick filaments during myofibrillogenesis (Whiting et al., 1989; Fulton and Isaacs, 1991; Trinick, 1994). The recent determination of the complete human titin sequence demonstrated conclusively that the protein has a complex modular architecture (Labeit et al., 1990, 1992; Gautel et al., 1993; Kolmerer and Labeit, 1995) (see Fig. 1). In human cardiac titin, one of the smallest isoforms, about 240 repeated modules of ~100 residues, equally divided between types I and II, account for more than 80% of the total sequence. The type II (Ig-like) modules are representative of the most diverse known class of modules in animals and occur frequently along the whole titin molecule as well as in other related muscle proteins (Benian et al., 1989). In the A-band about 35 type II modules alternate with 90 type I modules (fibronectin III-like) to form a very regular 11-domain super-repeat pattern (-II-I-I-II-I-I-I-II-I-I-I-). Within the M-line, 10 type II modules are separated by nonrepetitive "linker" sequences. Finally, about 50 Ig-like modules are arranged in tandem for the greater part of the elastic I-band region, occasionally flanked by unique insertion sequences with no detected homologies in the database (Kolmerer and Labeit, 1995). Because of this modularity, we decided to explore the molecular basis of the properties of titin (including its elasticity and extensibility) by dissecting it into units small enough to be structurally characterized in full detail (Politou et al., 1994b; Musco et al., 1995). We have recently determined the solution structure of one of the carboxy-terminal type II domains (Pfuhl and Pastore, 1995; Pfuhl et al., 1995), which has the immunoglobulin I

Received for publication 1 June 1995 and in final form 22 August 1995.
Address reprint requests to Dr. Anastasia S. Politou, EMBL, Meyerhofstrasse 1, D69012 Heidelberg, Germany. Tel.: 49-6221-387551; Fax: 46-6221-387306; E-mail: politou@embl-heidelberg.de.

0006-3495/95/12/2601/10 $2.00

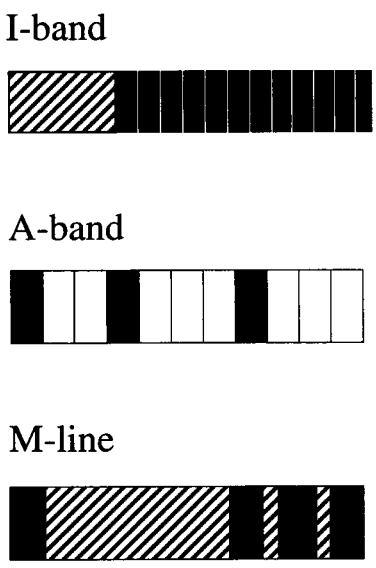

FIGURE 1 Schematic representation of the modular architecture of titin in different regions of the sarcomere. The scheme is adapted from Kolmerer and Labeit (1995). Filled and open boxes indicate Ig-like and fibronectin-like modules, respectively. Diagonally striped boxes represent nonrepetitive linker sequences. In both the I-band and the A-band, the end of each consensus sequence appears to be directly attached to the beginning of the next.

(i.e., intermediate) fold (Harpaz and Chothia, 1994). It is reasonable to expect that all type II modules have the same basic immunoglobulin I fold because they share the same key residues common to the entire subclass of muscle proteins and essential for this fold. However, our previous work has indicated that the stability of modules varies considerably in a position-related manner (Politou et al., 1994a,b). This variation in stability is of particular interest because titin modules in different regions of the sarcomere have different functional and mechanical tasks to perform. The M-line, for example, serves as a rigid anchoring plane for the thick filament and, as such, must need very stable constituent modules. On the other hand, complete reversibility of unfolding might be the major requirement for the modules of the extensible and presumably elastic I-band region. Therefore, the investigation of stabilities of modules from very different locations along the sarcomere is important in its own right.

It is neither reasonable nor feasible to determine directly the tertiary structure of each of the >100 Ig-like modules found in titin, so the results of this stability study serve another important purpose: when combined with the information from the tertiary structure of single modules and module pairs, and homology modeling, they could provide the basis for a relatively well supported and reliable structural description of intact titin. Also, understanding the way in which module stability is affected by intrinsic structural determinants and by contributions from the environment will significantly contribute to our general understanding of the ever-expanding family of "mosaic" proteins. This type of analysis has been used recently in similar cases with very interesting results (Novokhatny and Ingham, 1994; Mayr et al., 1994). In this paper we report the results of a detailed stability survey of representative titin modules from different regions of the sarcomere and discuss their implications for models of the elasticity and extensibility of the molecule.

MATERIALS AND METHODS

Materials

Complementary DNAs (cDNAs) coding for various titin Ig-like (type II) domains from the I-band, A-band, and M-line regions of human cardiac titin were isolated by polymerase chain reaction (Saiki et al., 1985) as described before (Labeit et al., 1992; Gautel et al., 1993; Kolmerer and Labeit, 1995). The module boundaries were selected on the basis of an extensive sequence alignment of all type II titin modules (Labeit et al., 1990; Politou et al., 1994a). The DNA fragments obtained were subcloned into the pET8c vector (Studier et al., 1990) and fused amino-terminally with an oligonucleotide linker encoding a His_6 tag sequence, introducing an additional two serine residues in the linker. After induction of transformed BL21 [DE3] pLysE cells (Studier and Moffat, 1986) with 0.3 mM isopropyl [β]-D-thiogalactoside for 4 h, the harvested cell pellet was treated with lysozyme at 20 μg/ml and sonicated in 50 mM sodium phosphate, pH 8.0, 150 mM NaCl, 0.1% Triton X-100 (buffer A). After centrifugation at 25,000 $\times$ g and washing, the soluble supernatant was fractionated by metal chelate affinity chromatography on Ni^{2+}-nitrilotetraacetic acid agarose (Qiagen) essentially as described by LeGrice and Grueninger-Leitch (1990). The washed column was developed with a gradient of 0–200 mM imidazole, 20 mM [β]-mercaptoethanol at pH 7, and pure fractions were pooled, diluted to 100 μg/ml, dialyzed against several buffer changes of 20 mM Tris/acetate, pH 8.0, 1 mM EDTA, 0.5 mM phenylmethanesulfonyl fluoride, and passed over Q-sepharose equilibrated in the dialysis buffer. Unbound fractions containing titin domains judged pure by sodium dodecyl fluoride-polyacrylamide gel electrophoresis (Laemmli, 1970) were dialyzed against the appropriate assay buffers and concentrated with an Amicon concentrator. The buffers used for the unfolding curves were 10–20 mM glycine (pH = 2.0–2.8 and 9.0–10.0), citrate/phosphate (pH = 2.5–3.5), acetate (pH = 4.0–5.0), phosphate (6.5–7.8), 3[*N*-morpholino]propanesulfonic acid, sodium salt (7.0–7.6), and Tris/acetate (7.1–9.5).

Fluorescence spectroscopy-urea denaturation studies

The intrinsic fluorescence of all modules decreases and the position of the maximum emission wavelength undergoes a red shift of at least 20 nm upon denaturation, so that fluorescence spectroscopy can conveniently be used to monitor the unfolding. The intensity of fluorescence emission was monitored at 305, 309, 316, 352, and 357 nm with an excitation wavelength of 293 nm on an SLM-Aminco Bowman Series 2 spectrofluorimeter with a bandpass of 4 nm for both excitation and emission. Urea stock solutions in the concentration range 0–10 M were prepared gravimetrically in volumetric flasks with "ultrapure" urea (Schwarz/Mann Biotech) and the appropriate buffer, and were stored at −20°C after being divided into 750-μl aliquots with an Eppendorf multipette. Protein stock solutions were added to these so that a final protein concentration of 50–70 μg/ml was reached. The solutions were incubated at 25°C for 10–12 h before the measurement. Fluorescence spectra were recorded in 0.5-cm quartz cuvettes thermostatted at 25 $\pm$ 0.1°C. The temperature was monitored throughout the experiment by measuring the temperature of an adjacent cuvette in the cell holder. After the fluorescence measurements, the pH of four or five solutions near the midpoint of the transition was recorded on a PHM93 radiometer pH meter after a double buffer adjustment; the average was considered as the pH of denaturation. A two-state model of

denaturation, in which only the denatured and the native states are considered to be significantly populated, was used to analyze the curves. Such an assumption is supported by the single-step shape of the unfolding curves. The free energy of unfolding, ΔG, may be calculated from the points in the transition region using

$$\Delta G = -RT \ln K = -RT \ln(f_u/f_f) = -RT \ln\left[\frac{y_f - y}{y - y_u}\right], \quad (1)$$

where R is the gas constant; T is the absolute temperature; K is the equilibrium constant; f_f and f_u represent the fraction of protein present in the folded and unfolded conformations, respectively; y is the observed fluorescence intensity at the selected wavelength; and y_f and y_u are the values of the fluorescence intensities characteristic of the folded and unfolded conformations, respectively (Pace et al., 1989). Assuming a linear dependence of ΔG on urea concentration the data can be fitted, as has been shown for many proteins (Tanford, 1968; Pace, 1986), to the equation

$$\Delta G = \Delta G(H_2O) - m[U], \quad (2)$$

where $\Delta G(H_2O)$ is the value of ΔG at 25°C in the absence of the denaturant (known as conformational stability), m is related to the increase in the degree of exposure of the protein upon denaturation, and [U] is the urea concentration. Assuming that both y_f and y_u are linearly dependent on urea concentration (i.e., $y_f = a_f + m_f[U]$ and $y_u = a_u + m_u[U]$) we find from Eqs. 1 and 2 that

$$y = \frac{(a_f + m_f[U]) + (a_u + m_u[U])\left(\exp\left[-\frac{\Delta G(H_2O)}{RT} - \frac{m[U]}{RT}\right)\right]}{1 + \exp[-(\Delta G(H_2O)/RT - m[U]/RT)]}, \quad (3)$$

where a_f and a_u are the intercepts, and m_f and m_u are the slopes of the pre- and the post-transition baselines, respectively. For constant baselines $m_f = m_u = 0$. The entire unfolding curve can then be fitted to Eq. 3. Alternatively (or additionally), the value for $[U]_{1/2}$ (the concentration of urea at which 50% of the protein is denatured) can be calculated by fitting the denaturation curve to Eq. 4 derived from Eq. 3, using $\Delta G(H_2O) = m[U]_{1/2}$:

$$y = \frac{(a_f + m_f[U]) + (a_u + m_u[U])\left(\exp\left[\frac{m([U] - [U]_{1/2})}{RT}\right]\right)}{1 + \exp[m([U] - [U]_{1/2})/RT]}. \quad (4)$$

The entire curves obtained from the denaturation experiment were fitted using the nonlinear regression analysis program Kaleidagraph (Abelbeck Software), and all seven parameters of Eqs. 3 and 4 were obtained with their standard errors.

Circular dichroism-thermal unfolding

Circular dichroism (CD) spectra in the far ultraviolet were recorded on a Jasco J-710 spectropolarimeter, fitted with a thermostatted cell holder connected to a Neslab RTE-110 water bath. The instrument was calibrated with a 0.10% aqueous solution of D-10-camphor-sulfonic acid. Thermostatted quartz cuvettes (Hellma) with path lengths in the range 0.01–2.0 mm were used, depending on the protein concentration, so that the combined optical density (OD) of cell, sample, and solvent was kept to less than 1 over the measured range. Typically, spectra were recorded with 0.2 nm resolution and were baseline-corrected by subtraction of the appropriate buffer spectrum. Thermal denaturation of the modules was monitored by following the change in the far-UV CD spectrum with temperature increasing at 20°C/h. Covered cuvettes with a path length of 1 mm were used in all cases for protein concentrations close to 0.2 mg/ml. The temperature inside the cuvette holder was checked constantly with a flexible temperature sensor. Our analysis of the resulting thermal denaturation curves was based on a two-state approximation (Becktel and Schellman, 1987). The curves were fitted to an equation analogous to Eq. 4 corresponding to thermal denaturation, and the value of the melting temperature (T_m) (midpoint of thermal transition) was obtained with its standard error.

Nuclear magnetic resonance spectroscopy

One-dimensional (1D) and two-dimensional (2D) nuclear Overhauser-effect ^1H nuclear magnetic resonance (NMR) spectra were recorded for all modules used in the present study from samples containing approximately 1 mM protein in 92% H_2O/8% D_2O and 20 mM acetate buffer at pH 4.4 and 27°C. All spectra were acquired on a Bruker AMX-500 spectrometer. For 2D experiments, phase-sensitive mode (time-proportional phase incrementation) with pre-irradiation of the water resonance was used. A mixing time of 120 ms was used for the nuclear Overhauser-effect spectra. Data were processed on a Bruker X-32 data station using UXNMR software. For the thermal unfolding experiment, a series of 1D spectra of ~0.7 mM solutions of protein in 20 mM sodium phosphate buffer at pH 7.5 were recorded from 20°C up to at least 5°C above complete unfolding with 5°C steps. The temperature of the probe was calibrated beforehand with an ethylene glycol standard. One hundred twenty-eight scans were used for each measurement at an interval of about 20 min for the temperature to stabilize. To avoid aggregation or chemical modification effects which would affect reversibility, the unfolded protein was kept at high temperatures for a short time. Refolding was achieved by rapid cooling.

Determinations of pK_a of histidine residues by NMR

The pK_a values of the histidine residues of the amino-terminally added His_6 tag were determined at 25°C by NMR titration. One-dimensional NMR spectra were recorded from samples containing 0.8 mM protein and 50 mM NaCl in 99.99% D_2O on the Bruker 500 MHz spectrometer at 25 ± 0.1°C. Two hundred fifty-six transients were averaged for each spectrum. Before the experiment started, the amide protons were allowed to exchange almost completely by prolonged dialysis against D_2O/50 mM NaCl at pD 9.3. The pD was adjusted in the course of the titration with DCl and measured on a PHM93 Radiometer pH meter calibrated against standard buffers but not corrected for the isotope effect. The resonances of the imidazole ring protons of the six histidine residues in the amino-terminal tag were dispersed by no more than 0.01 ppm and titrated in an identical way with changing pD. The chemical shifts of the $C^{\epsilon 1}$ proton (often designated as C2) were fitted to the equation of a single ionization equilibrium and the value of pK_a was thus determined. Chemical shifts are quoted relative to 4,4-dimethyl-silapentane-1-sulfonate. The value of the pK_a was also determined for the denatured protein in the presence of 9.5 M perdeuterated urea/50 mM NaCl in D_2O at 25 ± 0.1°C as described above. The pK_a of a single histidine (purchased from Sigma) was determined independently by NMR under conditions identical to those used for the protein to quantitate the effect of D_2O on the measured values of pK_a.

RESULTS

All modules are autonomously and similarly folded

All far-UV CD spectra recorded at room temperature are similar and typical of β-sheet proteins (see Fig. 2 *a*). The fluorescence emission spectra are all dominated by the intrinsic fluorescence of the unique tryptophan, with wavelength and intensity characteristic for a tryptophan well buried in the protein core (Fig. 2 *b*). The 1D and 2D NMR spectra of all the modules studied are diagnostic of folded, nonaggregated proteins sharing the same folding pattern.

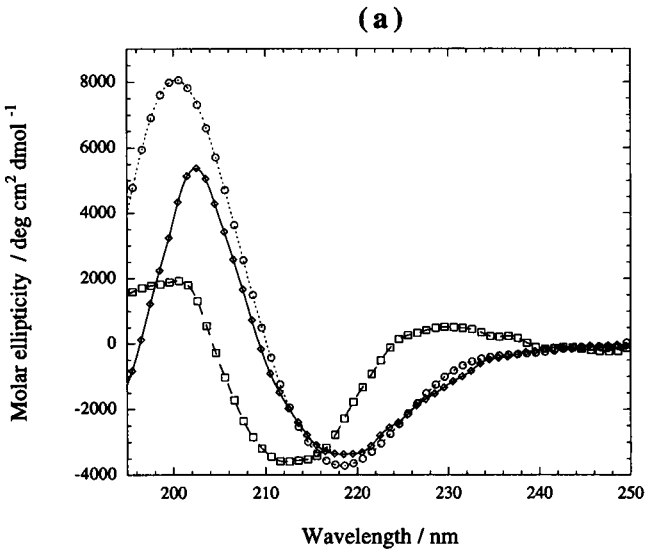

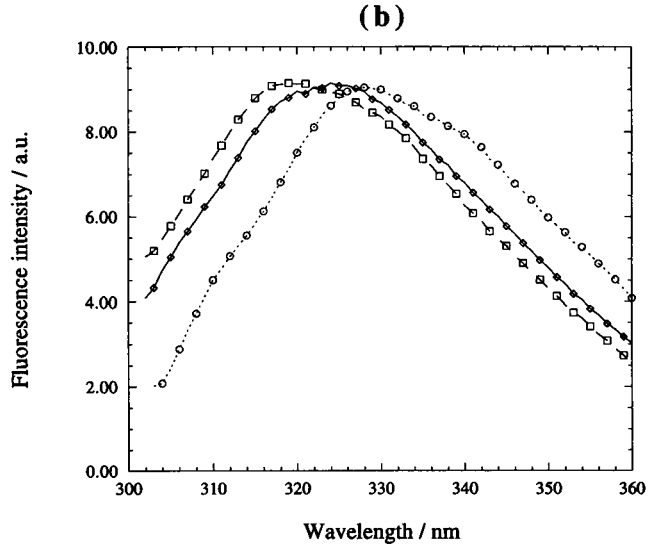

FIGURE 2 Normalized far-UV CD spectra (*a*) and fluorescence emission spectra (*b*) of titin modules I27 (*dashed line with squares*), A2 (*solid line with diamonds*) and M5 (*dotted line with circles*) at pH = 7, 20 mM phosphate buffer, 25°C.

Modules from the A-band are intrinsically the least stable

All thermal and chemical denaturation curves were analyzed by postulating a two-state mechanism of unfolding, supported by the single-step shape of the curves (see Figs. 3 and 4). Only in the case of module M5 (vide infra) could the thermal denaturation (but not the chemical denaturation) be more complex. Tables 1 and 2 summarize the results of the thermal and chemical denaturation study. All relevant thermodynamic parameters are included, together with their standard errors. The most objective parameters of the ones listed in Table 2 are the melting temperature, T_m, and $[U]_{1/2}$, i.e., the midpoints of the thermal and chemical denaturation

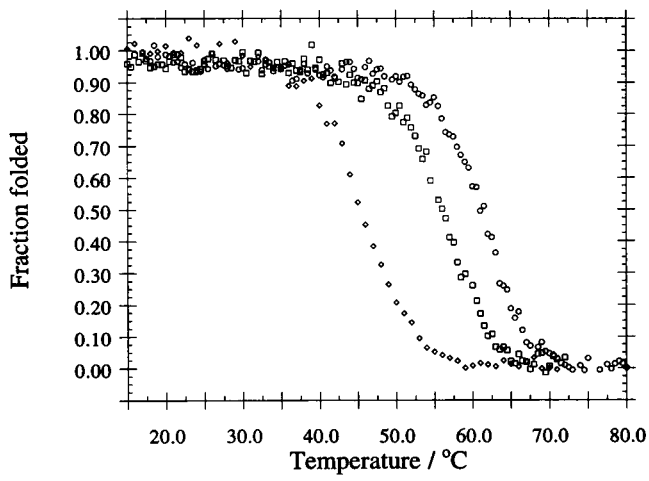

FIGURE 3 Thermal denaturation curves of the titin modules M7 (○), I55 (□), and A2 (◇) in 20 mM acetate buffer, pH = 4.2. Thermal unfolding was monitored by CD. Data shown are normalized.

curves, respectively, because their values do not depend to a great extent on the unfolding mechanism or the method of analysis used and can thus be determined quite accurately. In contrast, m (the slope of the unfolding curve) is not measured directly, and deviations from a two-state unfolding mechanism can generally affect its values significantly. Small errors in m can lead to large errors in $\Delta G(H_2O)$ because of the long extrapolation from the transition region to [U] = 0 (Jackson et al., 1993). However, the values of $\Delta G(H_2O)$ per se give an overall estimate of the stability of the protein and, as such, are quite useful, especially when differences in conformational stability among similar proteins are of more interest than their absolute values, as in our case. There is a certain danger in trying to draw conclusions about the conformational stabilities of different proteins based strictly on the midpoints of the unfolding curves (Pace et al., 1989); indeed, there are proteins with similar

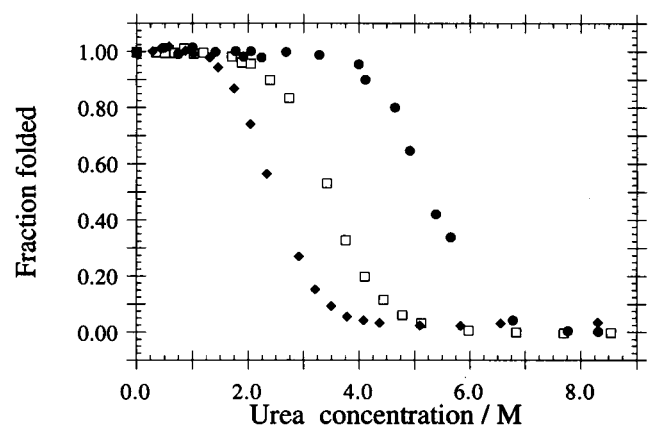

FIGURE 4 Urea-induced equilibrium unfolding of the titin modules I28 and A2 and of the CD2 domain 1 at pH = 7.2, 20 mM phosphate buffer, 25°C. I28 (◆); A2 (□); CD2 domain 1 (●). Unfolding was monitored by the intrinsic fluorescence intensity at 309 nm after excitation at 293 nm. These plots show normalized data.

TABLE 1 Thermal stability of titin modules

Module*	pI‡	pH§	T_m¶ (°C)
Z1	7.99	4.1	64.2 (0.2)
		7.2	69.4 (0.1)
I10	6.60	4.0	52.2 (0.4)
		7.1	60.1 (0.2)
I11	8.46	4.1	32.1 (0.9)‖
		7.2	35.3 (0.4)‖
I27	6.34	4.1	73.4 (0.2)
		7.3	72.6 (0.1)
I28	6.51	4.1	25.9 (0.5)‖
		7.2	54.1 (0.3)
I29	7.38	4.2	44.1 (0.1)
		7.1	54.0 (0.1)
I30	8.37	4.3	59.3 (0.1)
		7.4	61.1 (0.1)
I55	7.38	4.3	57.1 (0.2)
		7.1	67.8 (0.2)
A1	7.95	4.2	43.9 (0.1)
		7.1	46.1 (0.2)
A2	10.12	4.1	45.6 (0.2)
		7.1	50.6 (0.2)
A64	7.76	4.1	33.6 (0.5)
		7.1	45.7 (0.2)
M1	5.53	4.0	57.1 (0.4)
		7.1	62.2 (0.5)
M5	7.22	4.2	59.3 (0.3)
		7.3	68.8 (0.5)
M7	8.66	4.1	61.9 (0.2)
		7.1	70.0 (0.9)
	5.53	4.0	57.1 (0.4)
		7.1	62.2 (0.5)
CD2 (I)	7.53	4.0	72.0 (0.2)
		7.2	64.3 (0.2)

* Name of module. The capital letter preceeding the number of the module denotes position on the sarcomere, i.e., A-band (A), M-line (M), I-band (I), Z-disk (Z).

‡ Isoelectric point estimated on the basis of the sequence.

§ Buffers used are 20 mM sodium acetate (for pH 4) and 20 mM sodium phosphate (for pH 7).

¶ Melting temperature estimated from the thermal denaturation curves, as described in detail under Materials and Methods.

‖ This value could not be determined reliably, because the protein aggregated upon heating.

$\Delta G(H_2O)$ values that unfold at very different denaturant concentrations and proteins with markedly different $\Delta G(H_2O)$ values that "melt" at about the same temperature. Inspection of Tables 1 and 2, however, shows that this is not true in our case, probably because the proteins compared are related and their m values are very similar. The same conclusions can be drawn about the relative stabilities of the modules, irrespective of the thermodynamic parameter ($[U]_{1/2}$, T_m, or $\Delta G(H_2O)$) that one decides to select as the basis for the comparison; they vary considerably in a manner related to their locations along the titin molecule.

Finally, one should note that despite the sometimes very high melting points, the modules are generally characterized by $\Delta G(H_2O)$ values that are relatively low for globular proteins. The method we used to analyze the chemical denaturation curves, which is known to yield the lowest estimates of the conformational stabilities, could account in part for these low values. Most probably, however, they represent a real, intrinsic feature of the titin modules. To address this question, we also studied CD2 domain 1, which is another module of the Ig superfamily with the same type of fold as the titin modules (Driscoll et al., 1991; Jones et al., 1992). We determined its stability with the same methodology and found it to be very similar to that of the most stable titin domains (Tables 1 and 2) and therefore higher than the average.

Similar low $\Delta G(H_2O)$ values, derived mainly from calorimetric data, have been found by Alexander et al., (1992) for the small "B" domains of protein G and by Novokhatny and Ingham (1994) for the type I finger modules of fibronectin. It thus seems that there is a general tendency of small domains to have high melting temperatures and relatively low conformational stabilities, which was attributed by the groups mentioned above to the very flat and shallow ΔG versus T profile these proteins tend to have as a result of small ΔC_P values (heat capacity difference between folded and unfolded state at constant pressure).

The amino-terminal histidine tag appears to have no effect on the fold or on the stability

To check that the amino-terminally introduced His_6 tag has no specific effect on the structure or stability we determined the pK_a values of these histidines for module I27 by NMR in both the native and unfolded forms (Fig. 5). The average values of pK_a obtained by fitting the titration curves to a single ionization equilibrium were 6.56 ± 0.04 for the native proteins; 6.50± 0.02 for the denatured proteins; and 6.45 ± 0.02 for a free histidine residue in D_2O. In other words, the pK_a value was found to be identical to that of isolated histidine residues within experimental error and to those reported in the literature (6.6) for free histidines at the surface of proteins and in model peptides (Perutz et al., 1985; Sali et al., 1988; Sancho et al., 1992). Additional evidence comes from the chemical shifts of the histidine ring and α-protons, which have the values characteristic for random coil conformations and very little, if any, dispersion; from the absence of any NOE connectivities originating from the His_6 part of the molecule; and from the known tertiary structure of the M-line module M5 (Pfuhl and Pastore, 1995; Pfuhl et al., 1995).

Stability, but not fold, is pH dependent

The far-UV CD spectra of the modules were not affected by changing the pH in the range 3.8–9.1. Nor was a pH-dependent conformational change detected by NMR in this pH range. The only exception is seen with module I28, which is unfolded at room temperature and pH close to 4. The resistance to thermal denaturation, however, was affected significantly by changes in pH, as shown by the

TABLE 2 Conformational stabilities of titin modules at 25°C

Module*	pI*	pH*	$Urea_{1/2}^{\ddagger}$ (M)	$m^{\ddagger}$ (cal mol^{-1} M^{-1})	$\Delta G(H_2O)^{\ddagger}$ (kcal mol^{-1})
I11	8.46	7.2	3.82 (0.15)	786 (154)	3.00 (0.61)
I27	6.34	4.2	5.79 (0.05)	1272 (116)	7.36 (0.69)
I28	6.51	7.2	2.74 (0.02)	1410 (51)	3.87 (0.14)
I29	7.38	4.3	1.65 (0.04)	1549 (131)	2.55 (0.24)
I30	8.37	4.1	3.01 (0.05)	1465 (212)	4.42 (0.67)
Ab1	7.95	4.2	1.58 (0.04)	1121 (90)	1.77 (0.18)
		7.1	2.51 (0.09)	1044 (162)	2.62 (0.44)
Ab2	10.12	4.1	1.33 (0.02)	1794 (93)	2.38 (0.14)
		7.1	3.45 (0.02)	1275 (22)	4.40 (0.08)
M5	7.22	4.2	3.46 (0.04)	1330 (93)	5.56 (0.35)
		7.2	7.18 (0.03)	1418 (166)	10.19 (1.19)
CD2 (I)	7.53	4.3	5.60 (0.03)	1601 (100)	8.96 (0.60)
		7.3	5.26 (0.02)	1206 (50)	6.35 (0.26)

* Same notations as in Table 1.

‡ Calculated as described in detail under Materials and Methods.

values of the melting temperatures measured for two of the modules by CD at several pHs (Fig. 6). For the rest of the modules, the stability was assessed at physiological pH (~7) and at acidic pH (~4); the latter is more favorable for the NMR experiments because the amide protons exchange more slowly with the solvent and are therefore visible by NMR spectroscopy. The modules are more resistant to thermal denaturation around neutral pH. This trend is observed for all of the modules studied and it is more pronounced with some of them, such as I28, which at pH ~4 is unfolded at room temperature and reasonably stable at pH ~7. The same trend is observed when the values of the conformational stabilities (or $[U]_{1/2}$) are compared (Tables 1 and 2). Therefore it seems to be an intrinsic property of titin modules.

No correlation with the estimated isoelectric point (pI, also listed in Tables 1 and 2) could be detected.

Melting temperatures are independent of concentration

The thermal unfolding of the I-band modules I27 and I28 was also followed by NMR. Besides the obvious changes in the overall shape of the spectra, the resonances at low field (10–11 ppm) and high field (−0.5 to +0.5 ppm) were used to monitor the unfolding; those at low field originate from the $N^{\epsilon 1}$ proton of the indole side chain of the tryptophan residue, whereas those at high field are ring-current-shifted resonances of very conserved side-chain methyl protons very close in space to the tryptophan ring. The unique tryptophan is completely conserved among the titin type II modules and is a key residue for the Ig-type of fold, being part of the hydrophobic core of these proteins. The chemical shifts selected to follow the unfolding are therefore very sensitive probes of the tertiary structure (Fig. 7). The melting points thus determined were found to be identical within

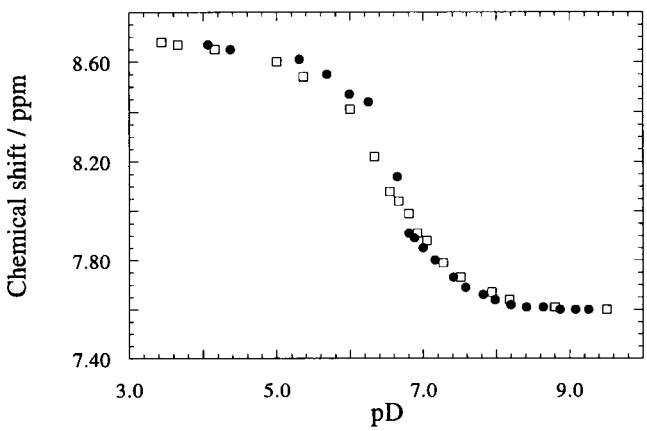

FIGURE 5 Titration of $C^{\epsilon 1}$ proton resonances of histidines in the aminoterminal His_6 tag of the titin module I27. Titration curves are shown for both the denatured protein (□) and the native protein (●) in D_2O/50 mM NaCl at 25°C.

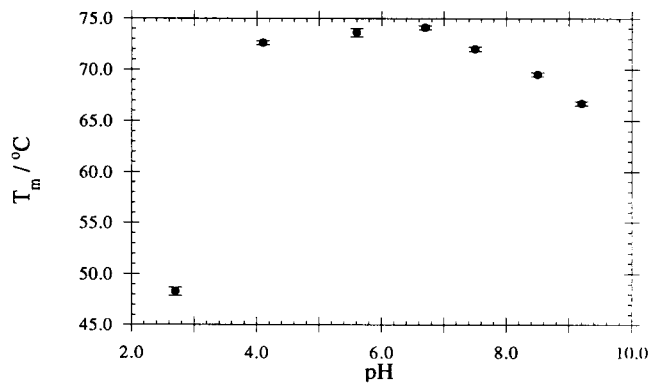

FIGURE 6 Melting temperature as a function of pH for module I27 in 20 mM buffer. T_m was determined by nonlinear regression analysis of thermal denaturation curves, as described in detail under Materials and Methods. The error bars indicate the standard error of the fit. The variation of the buffer pH with temperature has been taken into account.

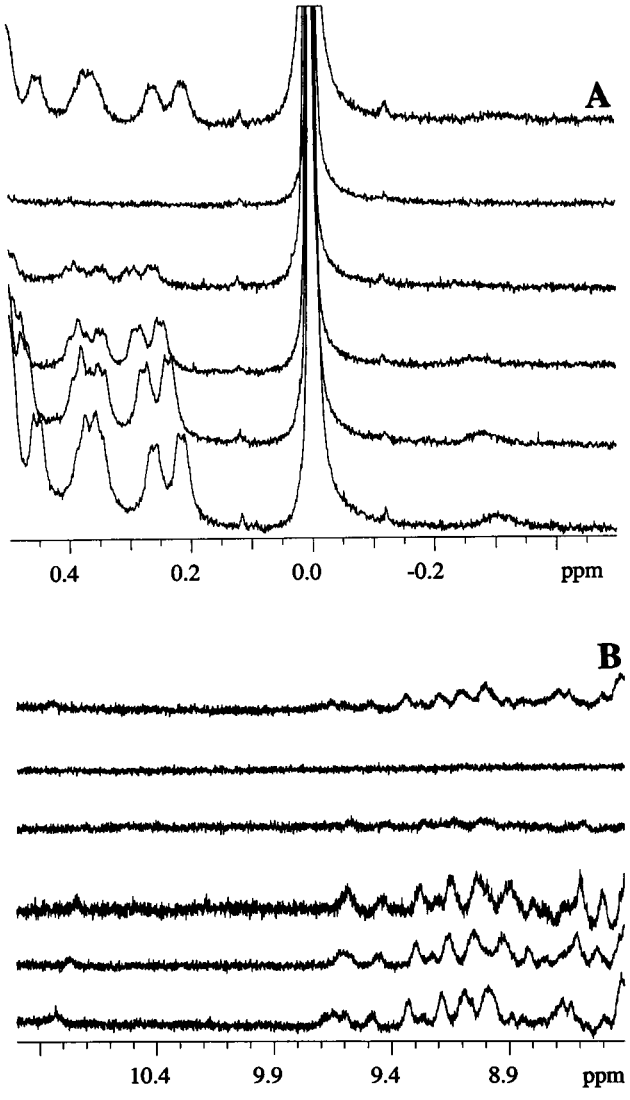

FIGURE 7 High-field (*A*) and low-field (*B*) regions of ^{1}H-NMR spectra of module I28 at temperatures (from bottom to top): 35, 42, 50, 56, 60, and again 35°C. The top trace shows the spectrum recorded at 35°C after the protein had been thermally unfolded. Spectra were recorded in 20 mM phosphate buffer, pH = 7.5 using 128 scans for each measurement (for details see Materials and Methods).

experimental error to those determined from the CD experiment (Table 1), although the concentrations used differ considerably (~0.2 mg/ml in the CD experiment and >6 mg/ml for the NMR titration). In both cases the unfolding was fully reversible and no appreciable aggregation was observed when the protein was recooled rapidly after denaturation.

Effect of ionic strength

Table 3 gives the melting temperatures of the I27 domain in several buffers. It is clear that the protein is destabilized slightly in the presence of phosphate buffer, whereas it is more stable in other "less ionic" buffers (such as 3[*N*-morpholino]propanesulfonic acid or Tris/acetate) and in pure water. The effect is not appreciable at low ionic strengths, but at phosphate concentrations greater than 50 mM there is a dramatic decrease (~12°C) in melting temperature.

TABLE 3 Effect of ionic strength on the stability of titin module I27*

Buffer	pH	T_m‡ (°C)
Water	7.0	76.0 (0.4)
10 mM phosphate	7.3	72.6 (0.2)
20 mM phosphate	7.3	72.0 (0.2)
50 mM phosphate	7.3	71.8 (0.2)
100 mM phosphate	7.3	59.2 (0.3)
200 mM phosphate	7.3	59.6 (0.3)
20 mM phosphate, 50 mM KCl	7.2	71.5 (0.2)
20 mM phosphate, 100 mM KCl	7.3	71.8 (0.2)

* Protein concentration in all cases was 20 μM.
‡ Calculated as described under Materials and Methods.

DISCUSSION

Implications about the mechanism of elasticity

The combined use of complementary spectroscopic techniques in the present work provided convincing experimental evidence that all of the titin type II modules studied fold independently in solution and share the same basic immunoglobulin I fold but have markedly different stabilities. Their stabilities seem to differ in a position-related way: the A-band domains are clearly the least stable; the M-line domains are all relatively stable; in the I-band titin, on the other hand, a larger variability of stabilities is observed. The higher stability of the M-line modules might be related to the rigidity required by this part of the titin molecule, which serves as an anchoring plane for the thick filament and to their being more autonomous, separated by "linker" sequences, in contrast to the A-band modules, which are always flanked and possibly further stabilized by the adjacent type I modules (see Fig. 1). In whole muscle, A-band modules are no doubt further stabilized by interactions with other thick-filament proteins.

The widely varying stabilities (but still in a range comparable to that covered by modules from other regions) that we observe for the I-band modules may have a direct bearing on the mechanism of titin elasticity, a topic of considerable current interest. Various models have been proposed; some require inter-domain interactions, whereas others posit entirely intra-domain rearrangements that one can summarize as "unfolding mechanisms" (Soteriou et al., 1993a; Erickson, 1994; L. Brady, personal communication).

There is a tendency in the literature about titin to confuse "elasticity" with "extensibility." Elasticity is a thermodynamically reversible material property. Any elastic specimen is necessarily also extensible, but extensibility is a much more loosely defined term. It means simply the ability to be extended with no implication of reversibility, thermo-

dynamic or otherwise. This distinction is of particular relevance to titin, which has been established beyond any reasonable doubt to be extensible, but is known to suffer irreversible damage if stretched too far. Titin is also presumed to be the "source" in moderately extended resting muscle of a nonlinear passive elasticity of unknown mechanism. In the intermediate regimen of fairly large extensions, titin shows some ability to recover (although only partially) over a time scale of hours. This is clearly not the physiologically relevant time scale for normal muscular activity. Therefore, we can only refer to experiments done in reversible conditions.

Entropic nature of muscle elasticity

The thermodynamic basis of passive muscular elasticity is often discussed using the Wiegand-Snyder equation:

$$f = \left(\frac{\partial U}{\partial \ell}\right)_T - T\left(\frac{\partial S}{\partial \ell}\right)_T. \quad (5)$$

Here f is the tension supported by the specimen, U is its internal energy, S its entropy, ℓ its length and T is the temperature. This equation has been widely used to determine experimentally the contributions of internal energy and entropy to an elastic force from its temperature dependence, the slope giving the entropy, and the intercept (at absolute zero) the internal energy. It has thus long been known that the passive elasticity of muscle is largely entropic in origin (Karrer, 1933). Current opinion is that titin makes a major contribution to this macroscopic property. However, it is the microscopic effects of the putative titin elasticity that excite the greater interest; titin is thought to provide the necessary restoring force preventing any tendency of thick filaments to miscenter during active contraction. It is important for what follows to know roughly how large this miscentering tendency is. Assuming that for every 15-nm increase in overlap between the thick and thin filaments 3 extra cross-bridges could be formed, but that only 20% of these are formed on average, and that the force each generates is about 5 pN, then the miscentering force has an equivalent (negative) spring rate of $\sim 20\% \times 3 \times 5$ pN $\div$ 15 nm = 200 μN m^{-1} per half thick filament. This has to be more than compensated by the set of titin molecules joining the other end of the thick filament to the distal Z-disc. The number of such molecules is not yet known with certainty but is thought on the grounds of symmetry to be either 3 or 6 (Maruyama, 1994). The stiffness of each titin molecule must therefore be greater than $\sim 200/3$ or $\sim 200/6$ μN m^{-1}.

Various models of titin elasticity

There is no experimental evidence proving that the immunuglobulin domains are responsible for the elasticity of titin, although such is commonly believed to be the case. Indeed, one proposed model of titin elasticity involves the complete unfolding of individual modules (Erickson, 1994). The argument is that the force supported by the unfolded domain is simply the free energy (Gibbs function) of unfolding divided by the increase in the amino- to carboxy-terminal distance: $f = \Delta G/\Delta \ell$. The calculation can be compensated with an estimate of the reduction of the entropy of the unfolded chain as it stretches, but it is hard to avoid the conclusion that the force necessary to initiate the unfolding (i.e., when $\Delta \ell$ is very small) must be extremely large, which accords well with intuition about such an all-β structure. For small extensions, when the configurational entropy is falling only slowly, but $\Delta \ell$ is rising from zero, the force calculated on this model actually decreases; in other words, the system has a negative dynamic stiffness. This is not impossible, but any control of the extension would be difficult because the modules could only be either fully folded or extended.

As it happens, the configurational entropy of the unfolded chain gives an independent and rather reliable estimate of the tensile force and its rate of increase. This can be done using the theory of rubber elasticity (Treloar 1975), which has been applied to polypeptide chains (Thomas, 1990). At physiological temperature (310 K) the characteristic spring rate is $\lambda \approx 61.4$ mN [residues] m^{-1} which must be divided by the number of residues in the unfolded chain (just over 100), giving ~ 600 μN m^{-1} for a single unfolded domain. This spring rate is close to the lower limit of useful stiffness as estimated above, but it applies only in the case of just one domain being unfolded. If further domains unfold, the value must be divided accordingly; this means that once a substantial miscentering occurs, there would be an ever-decreasing force trying to resist it, and it could not be prevented. Indeed, if a major fraction of the I-band domains were to unfold, the restraining force would be more than an order of magnitude too small to be of any use. These calculations thus suggest that the complete unfolding model does not properly explain the presumed elasticity of titin, although it may explain the remarkable extensibility under extreme conditions.

It is tempting to suggest that the elasticity may still be explained with a kinetic model such as that used for rubber elasticity. If each module may be regarded as a rigid link connected with some degree of rotational freedom to its neighbors, recalculation of the rubber-like tension is possible without assuming any unfolding of the individual domains. The result is an even lower tension than would be supported by the polypeptide chain if it were completely unfolded, in other words, nearly two orders of magnitude too small. This result follows from the fact that although the number of links is about 100 times smaller, the effective length of the link (closely related to the persistence length along the chain) is more than 10 times larger but appears squared in the formula (cf. equation 4.1 in Thomas, 1990). It is intuitively clear too: the tension arises from the reduction in entropy of the chain as it is stretched (cf. Eq. 5), but if the modules remain fully folded, the total configurational entropy is considerably less, and the tension drops commen-

surately. There are thus serious doubts that titin elasticity bears any deep resemblance to rubber elasticity. The fact that the length of the I-band does not fall to zero in relaxed muscle also argues against it.

Regardless of the folding patterns, it is impossible to find sufficient configurational entropy within the polypeptide chain of titin to explain the expected tensile force. A very obvious alternative candidate is the entropy of the surrounding cytosolic water: water in contact with a hydrofugal surface is more highly ordered than it would otherwise be, and this largely entropic effect is the accepted cause of the so-called hydrophobic forces commonly cited in studies of protein folding. It is easy to see that when the ΔG of unfolding of a titin domain is equivalent to only one or two hydrogen bonds (as our data show), then the extra exposure of even a small hydrophobic patch could easily involve a much greater change in the Gibbs function (the change in Gibbs function caused by the prevention of a hydrogen bond is thought to be between 3 and 7 kcal/mol, of which ~90% is attributable to the change in entropy (Schultz and Schirmer, 1979)). We propose a model in which adjacent titin modules are joined by hydrophobic hinge regions in such a way that when the titin is stretched, more hydrophobic surface becomes exposed to water, which becomes progressively more ordered. Our calculations done according to the method of Thomas (1990) indicate that a tensile force 100 times larger than that which could be caused by "internal" configurational entropy can easily be explained by this model, which would nevertheless not be strongly dependent on the precise folding pattern of the chain. Experimental support for this model could be provided by unfolding studies on multi-modular constructs as well as direct measurement of the forces involved in stretching of single titin molecules, which might then be compared with data obtained at the sarcomere level.

We thank Siegfried Labeit for communicating the titin I-band sequence before its publication; Mathias Gautel and Catherine Joseph for protein preparations; Luis Serrano and his group for the use of their fluorimeter; Simon Davis for the generous gift of the CD2 sample; and Mark Pfuhl, Leo Brady, and Harold Erickson for helpful discussions. We are indebted to Harold Erickson and K. W. Ranatunga for critical reading of the manuscript.

This work was supported by the Human Frontiers Science Programme. ASP was supported by a Bridge Senior Scientist Fellowship from the European Commission.

REFERENCES

Alexander, P., S. Fahnestock, T. Lee, J. Orban, and P. Bryan, P. 1992. Thermodynamic analysis of the folding of the streptococcal protein G IgG-binding domains B1 and B2: why small proteins tend to have high denaturation temperatures. *Biochemistry.* 31:3597–3603.

Becktel, W. J., and J. A. Schellman. 1987. Protein stability curves. *Biopolymers.* 26:1859–1877.

Benian, G. M., J. E. Kiff, N. Neckelmann, D. G. Moerman, and R. H. Waterston. 1989. Sequence of an unusually large protein implicated in regulation of myosin activity in *C. elegans*. *Nature.* 342:45–50.

Driscoll, P. C., J. G. Cyster, I. D. Campbell, and A. F. Williams. 1991. Structure of domain 1 of rat T lymphocyte CD2 antigen. *Nature.* 353: 762–765.

Erickson, H. P. 1994. Reversible unfolding of fibronectin type III and immunoglobulin domains provides the structural basis for stretch and elasticity of titin and fibronectin. *Proc. Natl. Acad. Sci. USA.* 91: 10114–10118.

Fulton, A. B., and W. B. Isaacs. 1991. Titin, a huge, elastic sarcomeric protein with a probable role in morphogenesis. *Bioessays.* 13:157–161.

Funatsu, T., E. Kono, H. Higuchi, S. Kimura, S. Ishiwata, T. Yoshioka, K. Maruyama, and S. Tsukita. 1993. Elastic filaments in situ in cardiac muscle: deep-etch replica analysis in combination with selective removal of actin and myosin filaments. *J. Cell Biol.* 120:711–724.

Fürst, D. O., M. Osborn, R. Nave, and K. Weber. 1988. The organization of titin filaments in the half-sarcomere revealed by monoclonal antibodies in immunoelectron microscopy: a map of ten nonrepetitive epitopes starting at the Z line extends close to the M-line. *J. Cell Biol.* 106: 1563–1572.

Gautel, M., K. Leonard, and S. Labeit. 1993. Phosphorylation of KSP motifs in the C-terminal region of titin in differentiating myoblasts. *EMBO J.* 12:3827–3834.

Harpaz, Y., and C. Chothia. 1994. Many of the immunoglobulin superfamily domains in cell adhesion molecules and surface receptors belong to a new structural set which is close to that containing variable domains. *J. Mol. Biol.* 238:528–539.

Horowits, R., K. Maruyama, and R. J. Podolsky. 1989. Elastic behavior of connectin filaments during thick filament movement in activated skeletal muscle. *J. Cell Biol.* 109:2169–2176.

Jackson, S. E., M. Moracci, N. el Masry, C. M. Johnson, and A. R. Fersht. 1993. Effect of cavity-creating mutations in the hydrophobic core of chymotrypsin inhibitor 2. *Biochemistry.* 32:11259–11269

Jones, E. Y., S. J. Davis, A. F. Williams, K. Harlos, and D. I. Stuart. 1992. Crystal structure at 2.8 Å resolution of a soluble form of the cell adhesion molecule CD2. *Nature.* 360:232–239.

Karrer, E. 1933. Kinetic theory of the mechanism of muscular contraction. *Protoplasma.* 18:475.

Keller, T. C. S., III. 1995. Structure and function of titin and nebulin. *Curr. Opin. Cell Biol.* 7:32–38.

Kolmerer, B., and S. Labeit. 1995. Titins, giant proteins in charge of muscle ultra-structure and elasticity. *Science.* In press.

Kurzban, G. P., and K. Wang. 1988. Giant polypeptides of skeletal muscle titin: sedimentation equilibrium in guanidine hydrochloride. *Biochem. Biophys. Res. Commun.* 150:1155–1161.

Labeit, S., D. P. Barlow, M. Gautel, T. Gibson, J. Holt, C. L. Hsieh, U. Francke, K. Leonard, J. Wardale, A. Whiting, and J. Trinick. 1990. A regular pattern of two types of 100-residue motif in the sequence of titin. *Nature.* 345:273–276.

Labeit, S., M. Gautel, A. Lakey, and J. Trinick. 1992. Towards a molecular understanding of titin. *EMBO J.* 11:1711–1716.

Laemmli, U. K. 1970. Cleavage of structural proteins during the assembly of the head of bacteriophage T4. *Nature.* 227:680–685.

LeGrice, S. F. J., and F. Grueninger-Leitch. 1990. Rapid purification of homodimer and heterodimer HIV-1 reverse transcriptase by metal chelate affinity chromatography. *Eur. J. Biochem.* 187:307–314.

Maruyama, K. 1994. Connectin, an elastic protein of striated muscle. *Biophys. Chem.* 50:73–85.

Maruyama, K., S. Kimura, H. Yoshidomi, H. Sawada, and K. Kikuchi. 1984. Molecular size and shape of β-connectin, an elastic protein of striated muscle. *J. Biochem. (Tokyo).* 89:701–709.

Mayr, E. M., R. Jaenicke, and R. Glockshuber. 1994. Domain interactions and connecting peptides in lens crystallins. *J. Mol. Biol.* 235:84–88.

Musco, G., C. Tziatzios, P. Schuck, and A. Pastore. 1995. Dissecting titin into its structural motifs: Identification of an α-helix motif near the titin N-terminus. *Biochemistry.* 34:553–561.

Nave, R., D. O. Fürst, and K. Weber. 1989. Visualization of the polarity of isolated titin molecules: a single globular head on a long thin rod as the M band anchoring domain? *J. Cell Biol.* 109:2177–2187.

Novokhatny, V. V., and K. C. Ingham. 1994. Domain structure of the Fib-1 and Fib-2 regions of human fibronectin. Thermodynamic properties of the type I finger module. *J. Mol. Biol.* 238:833–844.

Pace, C. N. 1986. Determination and analysis of urea and guanidinine hydrochloride denaturation curves. *Methods Enzymol.* 131:266–279.

Pace, C. N., B. A. Shirley, and J. A. Thomson. 1989. Measuring the conformational stability of a protein. *In* Protein Structure: A Practical Approach. T. E. Creighton, editor. Oxford, IRL Press. 311–330.

Perutz, M. F., A. M. Gronenborn, G. M. Clore, J. H. Fogg, and D. T. Shih. 1985. The pK_a values of two histidine residues in human haemoglobin, the Bohr effect, and the dipole moments of α-helices. *J. Mol. Biol.* 183:491–498.

Pfuhl, M., M. Gautel, A. S. Politou, C. Joseph, and A. Pastore. 1995. Secondary structure determination by NMR spectroscopy of an immunoglobulin-like domain from the giant muscle protein titin. *J. Biomol. NMR.* 6:48–58.

Pfuhl, M., and A. Pastore. 1995. Tertiary structure of an immunoglobulin-like domain from the giant muscle protein titin. *Structure.* 3:391–401.

Politou, A. S., M. Gautel, C. Joseph, and A. Pastore. 1994a. Immunoglobulin-type domains of titin are stabilized by amino-terminal extension. *FEBS Lett.* 352:27–31.

Politou, A. S., M. Gautel, M. Pfuhl, S. Labeit, and A. Pastore. 1994b. Immunoglobulin-type domains of titin: same fold, different stability? *Biochemistry.* 33:4730–4737.

Saiki, R. K., S. J. Scharf, F. Faloona, G. T. Mullis, G. T. Horn, H. A. Erlich, and N. Arnheim. 1985. Enzymatic amplification of β-globin genomic sequences and restriction site analysis for diagnosis of sickle cell anemia. *Science.* 230:1350–1354.

Sali, D., M. Bycroft, and A. R. Fersht. 1988. Stabilization of protein structure by interaction of α-helix dipole with a charged side chain. *Nature.* 335:740–743.

Sancho, J., L. Serrano, and A. R. Fersht. 1992. Histidine residues at the N- and C-termini of α-helices: perturbed pK_as and protein stability. *Biochemistry.* 31:2253–2258.

Schultz, G. E., and R. H. Schirmer. 1979. Principles of Protein Structure. Springer Verlag, New York. 33–38.

Soteriou, A., A. Clarke, S. Martin, and J. Trinick. 1993a. Titin folding energy and elasticity. *Proc. R. Soc. London B.* 254:83–86.

Soteriou, A., M. Gamage, and J. Trinick. 1993b. A survey of interactions made by the giant protein titin. *J. Cell Sci.* 104:119–123.

Studier, F. W., and B. A. Moffat. 1986. Use of bacteriophage T7 RNA polymerase to direct selective high-level expression of cloned genes. *J. Mol. Biol.* 189:113–130.

Studier, F. W., A. H. Rosenberg, and J. W. Dubendorff. 1990. Use of T7 RNA polymerase to direct expression of cloned genes. *Methods Enzymol.* 185:62–89.

Tanford, C. 1968. Protein denaturation. *Adv. Protein Chem.* 23:121–182.

Thomas, D. J. 1990. The entropic tension of protein loops. *J. Mol. Biol.* 216:457–463.

Treloar, L. R. G. 1975. The Physics of Rubber Elasticity. Clarendon Press, Oxford. 24–41.

Trinick, J. 1994. Titin and nebulin: protein rulers in muscle? *Trends Biochem. Sci.* 19:405–409.

Vinkemeier, U., W. Obermann, K. Weber, and D. O. Fürst. 1993. The globular head domain of titin extends into the center of the sarcomeric M band. cDNA cloning, epitope mapping and immunoelectron microscopy of two titin-associated proteins. *J. Cell Sci.* 106:319–330.

Wang, K. 1985. Sarcomere-associated cytoskeletal lattices in striated muscle. Review and hypothesis. *Cell Muscle Motil.* 6:315–369.

Whiting, A., J. Wardale, and J. Trinick. 1989. Does titin regulate the length of muscle thick filaments? *J. Mol. Biol.* 205:263–268.